Anti-CD20 Treatment Effectively Attenuates Cortical Pathology in a Rat Model of Widespread Cortical Demyelination

Michaela T Haindl
Medical University of Graz: Medizinische Universitat Graz https://orcid.org/0000-0003-0219-8535
Muammer Üçal
Medical University of Graz: Medizinische Universitat Graz
Benjamin Klaus
Medical University of Graz: Medizinische Universitat Graz
Lennart Tögl
Medical University of Graz: Medizinische Universitat Graz
Jana Dohrmann
Medical University of Graz: Medizinische Universitat Graz
Milena Z Adzemovic
Karolinska Institute: Karolinska Institutet
Christian Enzinger
Medical University of Graz: Medizinische Universitat Graz
Sonja Hochmeister (sonja.hochmeister@medunigraz.at)
Medical University of Graz https://orcid.org/0000-0002-3925-6455

Research

Keywords: Progressive Multiple Sclerosis, anti-CD20 therapy, rat model

Posted Date: February 23rd, 2021

DOI: https://doi.org/10.21203/rs.3.rs-229021/v1

Abstract

Background

Cortical demyelination represents a prominent feature of the multiple sclerosis (MS) brain, especially in (late) progressive stages. We recently developed a new rat model that reassembles critical features of cortical pathology characteristic to progressive types of MS. In persons affected by MS, B-cell depleting anti-CD20 therapy proved successful in the relapsing remitting as well as the early progressive course of MS, with respect to reducing the relapse rate and number of newly formed lesions. However, if the development of cortical pathology can be prevented or at least slowed down is still not clear. The main goal of this study was thus to increase our understanding for the mode of action (MOD) of B-cells and B-cell directed therapy on cortical lesions in our rat model.

Methods

For this purpose, we set up two separate experiments, with two different induction modes of B-cell depletion. Brain tissues were analyzed thoroughly using histology.

Results

We observed a marked reduction of cortical demyelination, microglial activation, astrocytic reaction and apoptotic cell loss in anti-CD20 antibody treated groups. At the same time, we noted increased neuronal preservation compared to control groups, indicating a favorable impact of anti-CD20 therapy.

Conclusion

These findings might pave the way for further research on the MOD of B-cells and therefore help to improve therapeutic options for progressive MS.

1. Introduction

The involvement of B-cells in Multiple Sclerosis (MS) has received increasing attention in the past few years following the success of B-cell-targeted therapy. Whilst the specific contribution of distinct subsets of B-cells to MS pathology remains unknown, in vitro experiments and animal studies pointed towards regulatory and inflammatory roles of several B-cell subsets, especially CD20 (cluster of differentiation 20) expressing cells (Barun and Bar-Or, 2012; Staun-Ram and Miller, 2017). Treatment of MS patients in the relapsing-remitting disease phase (RRMS) with anti-CD20 therapy resulted in a significant reduction of newly formed brain lesions and clinical relapses. This indicated an additional antibody-independent and pro-inflammatory function of B-cells (Barun and Bar-Or, 2012), by which they contribute to MS development and progression through targeting autoantigens, beside humoral antibodies, binding to brain cells, and thereby leading to tissue injury. Recent research also discussed leptomeningeal B-cell clusters to promote neuronal degeneration and demyelination, particularly in the later, progressive stages of the disease (Arneth, 2019).

The underlying pathogenic mechanisms of RRMS and progressive MS (PMS) differ. RRMS is characterized by inflammation and demyelination primarily driven by adaptive immunity, whilst in PMS, innate immune cells such as macrophages, dendritic cells, microglia and natural killer cells also play major roles, altogether emphasizing the multifaceted complexity in PMS pathogenesis. This difference could partially explain the fact that immunomodulatory or immunosuppressive drug formulations that successfully improve RRMS have been fairly ineffective in the treatment of PMS (Claes et al., 2015; 't Hart et al., 2017). Furthermore, chronic inflammation behind a closed blood-brain barrier (BBB) accompanied by microglial activation and continued involvement of T-cells and B-cells represent hallmark of PMS. However, clonally expanded plasma cells from MS patients produce antibodies directed against neurons and astrocytes but rarely against myelin components, suggesting that metabolic and energetic stress induced by inflammation could in fact precede demyelination and impede remyelination. Nevertheless, these antibodies caused demyelination in spinal cord explants *in vitro*, indicating an antibody-mediated pathology (Blauth et al., 2015; Faissner et al., 2019).

Prior to clinical trials, the positive effect of B-cell depletion on lesion formation had been mostly studied in classical animal models of experimental autoimmune encephalomyelitis (EAE), a model epitomizing the human pathology of RRMS quite well (Bouaziz et al., 2007; Matsushita et al., 2008; Weber et al., 2010). Although a beneficial effect of anti-CD20 therapy has also been discussed for PMS, the lack of available animal models resembling the respective pathological features have so far hindered a better understanding of B-cell involvement in demyelinating lesions of progressive MS types.

We have recently established an animal model that reconstitutes cortical demyelination characteristic for the progressive MS brain, resulting in widespread subpial demyelination (Ücal et al., 2017). In the present work, we investigated the effects of anti-CD20 treatment on cortical MS pathology using two different approaches in our model. In the first approach, we treated the animals with anti-CD20 *after* immunization against a recombinant myelin oligodendrocyte glycoprotein (MOG1-125). This experimental setup served as reenactment of the situation in MS patients under anti-CD20 therapy with already existing intrathecal antibodies, which diminishes all CD20 + B cell populations except those at the undifferentiated and fully differentiated stages (plasma cells), leaving the already established antibody titers unchanged. In the second approach, the rats were treated with the anti-CD20 antibody *before* MOG immunization, to check whether CD20 + B-cell populations play a role in building the autoimmune response itself and whether intrathecal antibodies are involved in the demyelination process. Control groups of both approaches were treated with respective isotype matched control antibodies.

2. Methods

2.1 Animals

Adult (10–12 weeks of age) male Dark Agouti (DA) rats (n = 30), obtained from a commercial vendor (Janvier, France), were housed in the animal facility of the Biomedical Research Institute at the Medical University of Graz under standard conditions with 12 h light/dark cycle. Food and water were provided *ad*

libitum. Animals' health status was checked at least once daily by qualified personnel. Following catheter implantation, they were moved to modified high top single cages to avoid damage to the catheter. All animal experiments were carried out under approval of the local authorities (Bundesministerium für Wissenschaft und Forschung; 66.010/0195-V/3b/2018). Animal numbers are listed in Table 1 in detail.

2.2 Experimental setup and Groups

All animals underwent intracerebral catheter implantation, as described previously (Ücal et al., 2017). After 2 weeks of healing of the blood brain barrier (BBB), animals were immunized with a recombinant MOG1-125 protein and received antibody treatment (anti-CD20 or isotype control) in two alternative orders: In Experiment 1, animals received anti-CD20 (E1, n = 9) or isotype control antibody (C1, n = 4) *after* MOG immunization. In Experiment 2, rats were treated with anti-CD20 (E2, n = 8) or isotype control antibody (C2, n = 3) *before* MOG immunization. Control animals (C2) received the isotype control antibody (n = 3). Control animals were implanted and immunized, but did not receive antibody nor cytokine (C0, n = 4). The timelines in Fig. 1 (a) and (b) gives an overview of the two approaches.

2.3 Catheter implantation

Animals were anaesthetized with intraperitoneal administration of a mixture of 0.03 mg/kg Fentanyl (Jansen-Cilag Pharma, Vienna, Austria), 0.6 mg/kg Midazolam (Erwo Pharma, Brunn am Gebirge, Austria) and 0.3 mg/kg Medetomidin (Orion Pharma, Espoo, Finland). Animals were well fixed on a stereotactic frame (David Kopf Instruments, Tujunga, CA, USA), where temperature stability was controlled using a rectal thermometer and a heating pad. A longitudinal incision was applied to head skin and the skull was exposed by removal of periosteum. A cranial hole with a diameter of 0.5 mm was drilled for the catheter over the right parietal cortex, 2.0 mm from the bregma and 2.4 mm from the medial suture. Three cranial holes with a diameter of 1 mm were drilled for screws, over the right and left parietal cortex at a few millimeters of distance from the first hole and plastic screws (PlasticsOne, Roanoke, VA, USA) were tightened by 2–3 full turns. The catheter (PlasticsOne, Roanoke, VA, USA) was cut to 2.0 mm length, inserted into the first opening and was placed into the cerebral cortex with the tip just above the corpus callosum. Catheter and screws were fixed with the help of dental cement (Heraeus Kulzer, Hanau, Germany). Afterwards, the skin was closed with resorbable sutures and anesthesia was antagonized with subcutaneous administration of a mixture of 0.105 mg/kg Flumazenil (Anexate; Roche Austria, Vienna, Austria) and 0.63 mg/kg Atipamezol (Antisedan; Orion Pharma). Animals were subcutaneously injected with enrofloxacin on the day of surgery (dose 7.5 mg/kg body weight; Baytril; Provet AG, Lyssach, Switzerland). The day after surgery, animals received another dose of enrofloxacin as well as a dose of (2% (v/v) Carprofen s.c. (Rimadyl; Zoetis Austria, Vienna, Austria) in physiological saline under brief anesthesia with isoflurane (AbbVie, Vienna, Austria) to control pain. Post-surgical recovery was uneventful in all cases. After 14 days, the catheter was completely healed in and the BBB was restored again (Ücal et al., 2017).

2.4 MOG immunization

Myelin oligodendrocyte glycoprotein (MOG, amino acids 1–125 from the N- terminus) used for EAE induction was expressed in Escherichia coli and purified to homogeneity by chelate chromatography (Amor et al., 1994). The purified protein, dissolved in 6 M urea, was dialyzed against phosphate buffered saline (PBS) to obtain a physiological preparation that was stored at − 70°C. Rats were briefly anaesthetized by inhalation of isoflurane and injected subcutaneously at the base of the tail with a total volume of 200 µl of 5 µg MOG diluted in saline, emulsified in incomplete Freund's Adjuvant (IFA; Sigma-Aldrich, Buchs, Switzerland). For the assessment of anti-MOG titers, peripheral blood was collected from the tail tip four weeks after immunization. Serum was harvested by 10 min centrifugation at 4000 g using a desktop centrifuge and stored at -80°C until usage.

2.5 Anti-CD20 Treatment

Animals were briefly anaesthetized by inhalation of isoflurane and injected intravenously at the base of the tail with 200 µL of 5 mg/ml antibody preparation (aCD20AB, Genentech, Roche Group) twice, with a time span of 7 days in between. Control animals were injected with the isotype control (anti-mouse IgG2a 5D2, company, country) at the same volume and concentration.

We set up two different approaches in order to attain our research goals. Both approaches were divided into two further groups where we used control antibodies (CAB; mouse IgG_{2a}, Leinco Technologies, Missouri, USA) instead of the aCD20AB. Since anti-CD20 therapy used for treating humans would not have comparable effects in the rat, we used a rat-specific research antibody (Genentech, Roche Group, anti-mCD20 mIgG2a 5D2).

2.6 Assessment of MOG Titer

MOG titers were assessed using enzyme linked immunosorbent assay (ELISA). In short, MOG (5 µL MOG/ml PBS) was coated on a 96-well plate (Nunc, Wiesbaden, Germany) and incubated for 1 h at 37°C. Then the plate was blocked with 1% bovine serum albumin (BSA; Serva, Heidelberg, Germany) in PBS for 1 h at room temperature. Afterwards the plate was incubated with rat sera (1:50) and standard for 2 h at 37°C. IgG specific horseradish peroxidase conjugated anti-rat antibody (1:10000) was used for detection. 2,2'-Azino-bis 3-ethylbenzthiazoline-6-sulfonic acid (ABTS) was added as substrate. Between these steps, the plate was washed three times with PBS/Tween. The optical density was measured at 405 nm wavelength.

2.5 Opening of the BBB

The BBB was opened by the time animals developed a MOG titer of 5–10 µg/mL or more, as assessed via ELISA. All animals received 2 µL of a cytokine mixture containing 500 µg/mL TNF-alpha (R&D systems, Abington, UK) and 300 U recombinant rat IFN-gamma/µL (PeproTech, London, UK), using a specific programmable syringe pump through the catheter (injection rate of 0.2 µL / min).

2.6 Sacrificing and tissue harvesting

Tissue samples were collected on day 15 after cytokine injection, at a time when we previously have shown that the cortical pathology reaches its maximum (Ücal et al., 2017), after euthanasia using overdose anesthesia by intraperitoneal injection of 1 ml pentobarbital sodium (Richter Pharma, Austria). Under deep anesthesia, the thorax was opened and the animals were transcardially perfused with 4% formaldehyde (Merck, Darmstadt, Germany) in phosphate buffered saline (PBS, pH 7.4). Brains, spinal cords and spleens were dissected and post-fixed in 4% FA for 24 hours at 4°C.

2.7 Neuropathology, immunohistochemistry and immunofluorescence

After routine embedding in paraffin, brains, spinal cords and spleens were cut in 1.5 µm sections. For immunohistochemistry (IHC), sections were dewaxed in xylol (Fisher Thermo Scientific, Schwerte, Germany), rehydrated and steamed for 1 h in citric acid (Merck) for antigen retrieval using a commercial steamer (Adzemovic et al., 2013; Ücal et al., 2017). To avoid unspecific binding, sections were blocked with 2.5% normal horse serum (Vector Laboratories Burlingame, CA, USA) at room temperature for 20 min, prior to incubation with the primary antibodies at 4°C overnight. For a detailed list of the used antibodies and dilutions, see the respective supplementary table 1 in the appendix. The enzymatic ImmPRESS System was utilized for detection with 3,3'diaminobenzidine-tetrahydrochloride (DAB, Sigma-Aldrich, Buchs, Switzerland) and counterstaining was performed with hematoxylin. After dehydration, slices were covered with a xylene based mounting medium (Shandon Consul-Mount, Fisher Thermo Scientific) and a coverslip. The slices immunostained with fluorescently labeled antibodies were washed with PBS after the incubation with fluorescent labeled secondary antibody (VectaFluor, Vector Laboratories) and covered with an aqueous mounting medium (Vectashield, Vector Laboratories) and a coverslip.

2.6 Quantitative histopathological evaluation

For the quantification of demyelination, microglial activation, astrocytic reaction, apoptotic cells and neurons, serial sections of the catheter insertion area were used. Demyelination was assessed by quantification of cortical loss of proteolipid protein (PLP) immunoreactivity for each hemisphere, using an optical grid at a magnification of 200x; values were then transformed to mm^2. Activated microglia (Iba-1), activated astrocytes (GFAP), apoptotic cells (Caspase-3) and neurons (NeuN) were assessed in three full optical grids in the cortex per hemisphere at a magnification of 200x and average values were then converted to cells/mm^2. Quantifications were performed by one blinded investigator.

2.7 Statistical analyses

All statistic calculations were performed using SPSS Statistics software (v23, IBM, USA), graphs were generated using Microsoft Excel 2010. All data is presented in box-whisker plots. Statistical significance of the observed differences was assessed with the Kruskal-Wallis H-Test, followed by a Mann-Whitney U test for pairwise comparisons. A difference with a p-value ≤ 0.05 was deemed statistically significant.

3. Results

3.1 Anti-CD20 treatment had an impact on anti-MOG titers

As expected, anti-CD20 treatment had a significant influence on building of the anti-MOG titers ($\chi^2(4) = 11.6$, $p < 0.02$). A pairwise comparison showed that anti-CD20 treatment before the MOG immunization resulted in significant attenuation in anti-MOG titers in comparison to the C0 control animals ($p = 0.017$), isotype control group (C2) ($p = 0{,}014$) as well as to the group that received anti-CD20 treatment after the MOG immunization (E1) ($p = 0.004$), whilst a comparable range of anti-MOG titers were observed in all other groups (Fig. 1c). Nevertheless, post-mortem analyses of CD45R- and CD20- immunoreactivities were equally diminished in both anti-CD20 treated groups in comparison with the controls that were treated with isotype control antibody, regardless of the timing of treatment (Fig. 1d).

3.2.1 Anti-CD20 treatment attenuates cortical demyelination

Animals treated with an isotype control antibody before or after MOG immunization showed a statistically significant cortical demyelination, substantiated by the reduction of PLP-immunoreactivity in both cerebral hemispheres, at 15 days after cytokine injection in comparison with the controls without cytokine injection (C1 ipsilateral (ipsi): $p < 0.02$, C1 contralateral (contra): $p < 0.01$, C2 ipsi: $p < 0.03$, C2 contra: $p < 0.02$) (Fig. 2a, b). Anti-CD20 treatment, however, prevented the cytokine-induced myelin loss to a large extent in both experimental groups (E1 ipsi: $p < 0.20$, E1 contra: $p < 0.23$, E2 ipsi: $p < 0.17$, E2 contra: $p < 0.18$; with no significant difference detectable between controls without cytokine injection and treatment group). It is worth to note that the preserved PLP-immunoreactivity was slightly stronger in the group that was treated with anti-CD20 before the MOG immunization (E2), when compared to those treated afterwards (E1). Representative images of PLP immunostaining are shown in Fig. 3.

3.2.2 Anti-CD20 treatment alleviates inflammatory reaction in cortex

Intracerebral cytokine injection into the animals that were treated with isotype control antibodies resulted in significant increases in the number of activated (Iba1+) microglia in both hemispheres compared with the C0 controls (C1: $p < 0.01$; C2: $p = 0.02$) (Fig. 2c, d). Concordant increases were observed in the number of reactive astrocytes (C1: $p < 0.02$; C2: $p = 0.05$) (Fig. 2e, f). Anti-CD20 treatment, however, effectively attenuated microglial activation (E1: $p < 0.01$, E2: $p = 0.02$) and astrocytic reaction (E1: $p < 0.01$, E2: $p = 0.04$) in both ipsi- and contralateral cerebral cortices in comparison with the corresponding controls. Together, these findings suggest that anti-CD20 treatment prevented cytokine-induced cortical demyelination through suppression of inflammatory responses. Representative immunofluorescent images of microglial activation are shown in Fig. 4a-c and of astrocytic reaction in Fig. 4d-f, respectively.

3.2.4 Anti-CD20 treatment reduced apoptotic cell death and neuronal loss

We have previously shown that the apoptotic cell death and neuronal loss were two other consequences of intracerebral cytokine injection following MOG immunization in our model (Ücal et al., 2017). In the current study, we observed significant increases in the number of Caspase-3 + cells in the cerebral cortices of animals that had been treated with isotype control antibody compared with the animals without a cytokine injection (both ipsi- and contralaterally; C1: $p < 0.01$, C2: $p = 0.02$) (Fig. 2g, h). Furthermore, there was a concordant reduction in cortical NeuN immunoreactivity in these animals (ipsilateral: $p < 0.02$ for C1 and C2; contralateral: $p < 0.01$ for C1 and $p = 0.02$ for C2). Anti-CD20 treatment, on the other hand, prevented the apoptotic cell death following a cytokine injection in the cerebral cortices in both treatment groups compared with the corresponding controls (both ipsi- and contralaterally; E1: $p = 0.008$, E2: $p = 0.01$). NeuN immunoreactivity, moreover, was preserved in both experimental groups (Fig. 2l, j). In none of the groups, a significant difference could be detected between C1 and C2 (p-values range between 0.06 and 1.00, see supplementary table 2 for details). Representative pictures of neuronal distribution via immunofluorescent staining are shown in Fig. 4g-i.

4. Discussion

Recent research has shown that B-cell depletion suppresses lesion development in experimental antibody-independent models of MS, therefore B-cells seem to play an important role in white matter lesion development, independent of auto-antibody production. There is also evidence for B-cells acting as antigen-presenting cells (APCs) and their involvement in the development and progression of MS appears likely. Anti-CD20 therapy can reduce the proliferation and activation of autoreactive CD4 + T-cells and IL-17 production in the CNS, resulting in a reduced clinical severity in animal models of MS (Matsushita et al., 2008; Kap, Laman and ‘t Hart, 2010; Monson et al., 2011). In our model of progressive MS, we demonstrated that administration of anti-CD20 therapy before or after immunization against MOG attenuated cortical demyelination induced by intracerebral injection of inflammatory cytokines. However, it should be noted that the effect was more pronounced in the group treated with anti-CD20 *before* the MOG immunization (E2 group). The anti-MOG-antibodies do play a role in our model and other experimental animal models like EAE (Mann et al., 2012), and depletion of B-cells effectively suppresses the building of immunization against MOG.

MOG immunization in DA rats *per se* frequently resulted in a slight temporary inflammation of limb joints, which spontaneously resolved in a couple of weeks. None of the anti-CD20 treated animals, however, showed such a reaction throughout the course of the experiments, indicating an anti-CD20-mediated suppression of overall peripheral autoimmune reactions, which are triggered by immunization similar to other autoimmune disease models (O’Neill, Glant and Finnegan, 2007; Korhonen and Moilanen, 2010; Meffre and O’Connor, 2019). It should, however, be noted that in all experimental groups, intracerebral injection of cytokines took place once the MOG titers reached a threshold level (6 µg/ml in most animals of the group). Therefore the observed effects did not solely depend on suppression of antibody production, although the prognostic clinical severity closely correlates to antibody titers in various autoimmune disease models, like EAE (Mann et al., 2012). Our findings allow us to conclude that the larger part of the mechanism is mediated via other B-cell functions, for example antigen presentation and

induction of innate immune responses. Remarkable reductions observed in microglial activation and astrocytic reaction in anti-CD20 treated animals further substantiated these assumptions.

In comparison to our previous investigations using the same animal model without any therapeutic intervention (Ücal et al., 2017), the control groups of the current study receiving a isotype matched control antibody (C1 and C2) showed less demyelination (PLP loss: 1.0 ± 0.2 (d15) vs 0.4 ± 0.2 (C1) and 0.3 ± 0.1 (C2), d15 animal without therapy and isotype antibody treated), suggesting a more favorable impact on the observed cellular patterns, although the demyelination was invariably distinctive compared to the anti-CD20 treated groups. This effect is, presumably, attributable to a similar phenomenon already known from the studies that have reported a beneficial impact of unspecific immunoglobulin therapy (e.g., Johnston and Hollingsworth, 2016). As a clinical standard therapy, unspecific antibodies obtained from blood preservations are used to treat several immune-mediated diseases to enable formation of unspecific complexes, which thereby inactivate pathogenic antibodies. Our isotype control antibody might have acted in a similar way (Helliwell and Coles, 2009).

A common theory regarding cortical pathology in MS is the consideration of unnoticed cortical damage, starting early in the disease course besides the obvious white matter lesion formation, slowly accumulating over decades by successively exhausting the regenerative capacity. In patients entering a progressive MS phase, amongst other numerous tissue changes, damage to the cortex including cortical demyelination has accumulated. Our data support the assumption, that anti-CD20 therapy - administered early in the disease course - could reduce, delay or even prevent cortical demyelination, as well as reduce the extent of apoptotic cell death, thereby promoting neuronal survival. The remarkably similar results of our both experimental approaches involving anti-CD20 therapy indicate that, in this context, cellular functions of B-cells seem to be much more important to disease progression than antibody production alone. This means that anti-CD20 therapy seems to have a positive effect on disease course, even when administered after disease onset and not only before (Mann et al., 2012). Given the wide use of CD20 antibody therapy in RRMS patients, time will tell if indeed the conversion rate to progressive MS or evolution of disability will diminish, as extrapolated from these observations.

5. Conclusion

Our results indicate a critical involvement of CD20 + B-cells on cortical lesion development, given the fact that in both experimental approaches cortical pathology was significantly attenuated upon anti-CD20 treatment, reflected in reduced myelin loss, astrocyte and microglial activation, apoptosis and neuronal loss. Furthermore, we show that the B-cell populations had a significant role in building autoimmunity against MOG. Finally our data demonstrate that already established intrathecal antibodies do not play a significant role in cortical demyelination in our animal model.

Abbreviations

APC – antigen presenting cells

BBB – blood brain barrier

DA – dark agouti

EAE – experimental autoimmune encephalomyelitis

GFAP – glial fibrillary acid protein
IFA – incomplete freund's adjuvands

IHC - immunohistochemistry

MOG – myelin oligodendrocyte glycoprotein

MS – multiple sclerosis

PBS – phosphate buffered saline

PLP – proteolipid protein

Declarations

Ethics approval and consent to participate: All animal experiments were carried out under approval of the local authorities (Bundesministerium für Wissenschaft und Forschung; 66.010/0195-V/3b/2018).

Consent for publication: Not applicable

Availability of data and material: Supporting Data and Information about material can be accessed by contacting one of the authors.

Competing interests: All authors have approved the final manuscript and declare no conflicts of interests. This work has not been published elsewhere.

Funding: This study was in part financially supported by Roche; the antibody was provided by Genentech. The pharmaceutical company however had no influence on study design and data interpretation.

Authors' contributions: MTH was responsible for histology, analyzed and interpreted the data and was the major contributor in writing the manuscript. MÜ was the specialist for surgery and animal handling and contributed to statistics. Main contribution of BK and LT was during surgery and animal handling. JD was mainly involved in histology and statistics. MZA and CE were main contributors to improve the final manuscript and SH was involved in all steps and is responsible for the cooperation and manuscript idea. All authors read and approved the final manuscript."

Acknowledgements Not applicable

References

't Hart, B. A. *et al.* (2017) 'A B cell-driven autoimmune pathway leading to pathological hallmarks of progressive multiple sclerosis in the marmoset experimental autoimmune encephalomyelitis model', *Frontiers in Immunology*, 8(JUL), pp. 1–14. doi: 10.3389/fimmu.2017.00804.

Adzemovic, M. Z. *et al.* (2013) 'Efficacy of vitamin D in treating multiple sclerosis-like neuroinflammation depends on developmental stage', *Experimental Neurology*, 249, pp. 39–48. doi: 10.1016/j.expneurol.2013.08.002.

Arneth, B. M. (2019) 'Impact of B cells to the pathophysiology of multiple sclerosis', *Journal of Neuroinflammation*. Journal of Neuroinflammation, 16(1), pp. 1–9. doi: 10.1186/s12974-019-1517-1.

Barun, B. and Bar-Or, A. (2012) 'Treatment of multiple sclerosis with Anti-CD20 antibodies', *Clinical Immunology*. Elsevier Inc., 142(1), pp. 31–37. doi: 10.1016/j.clim.2011.04.005.

Blauth, K. *et al.* (2015) 'Antibodies produced by clonally expanded plasma cells in multiple sclerosis cerebrospinal fluid cause demyelination of spinal cord explants', *Acta Neuropathologica*, 130(6), pp. 765–781. doi: 10.1007/s00401-015-1500-6.

Bouaziz, J. D. *et al.* (2007) 'Therapeutic B cell depletion impairs adaptive and autoreactive CD4 + T cell activation in mice', *Proceedings of the National Academy of Sciences of the United States of America*, 104(52), pp. 20878–20883. doi: 10.1073/pnas.0709205105.

Claes, N. *et al.* (2015) 'B cells are multifunctional players in multiple sclerosis pathogenesis: Insights from therapeutic interventions', *Frontiers in Immunology*, 6(DEC). doi: 10.3389/fimmu.2015.00642.

Faissner, S. *et al.* (2019) 'Progressive multiple sclerosis: from pathophysiology to therapeutic strategies', *Nature Reviews Drug Discovery*. Springer US, 18(12), pp. 905–922. doi: 10.1038/s41573-019-0035-2.

Helliwell, C. L. and Coles, A. J. (2009) 'Monoclonal antibodies in multiple sclerosis treatment: Current and future steps', *Therapeutic Advances in Neurological Disorders*, 2(4), pp. 195–203. doi: 10.1177/1756285609337827.

Johnston, S. L. and Hollingsworth, R. (2016) 'Immunoglobulin therapy', *Clinical Medicine, Journal of the Royal College of Physicians of London*, 16(6), pp. 576–579. doi: 10.7861/clinmedicine.16-6-576.

Kap, Y. S., Laman, J. D. and 't Hart, B. A. (2010) 'Experimental autoimmune encephalomyelitis in the common marmoset, a bridge between rodent EAE and multiple sclerosis for immunotherapy development', *Journal of Neuroimmune Pharmacology*, 5(2), pp. 220–230. doi: 10.1007/s11481-009-9178-y.

Korhonen, R. and Moilanen, E. (2010) 'Anti-CD20 antibody rituximab in the treatment of rheumatoid arthritis', *Basic and Clinical Pharmacology and Toxicology*, 106(1), pp. 13–21. doi: 10.1111/j.1742-7843.2009.00452.x.

Mann, M. K. *et al.* (2012) 'Pathogenic and regulatory roles for B cells in experimental autoimmune encephalomyelitis', *Autoimmunity*, 45(5), pp. 388–399. doi: 10.3109/08916934.2012.665523.

Matsushita, T. *et al.* (2008) 'Regulatory B cells inhibit EAE initiation in mice while other B cells promote disease progression', *Journal of Clinical Investigation*, 118(10), pp. 3420–3430. doi: 10.1172/JCI36030.

Meffre, E. and O'Connor, K. C. (2019) 'Impaired B-cell tolerance checkpoints promote the development of autoimmune diseases and pathogenic autoantibodies', *Immunological Reviews*, 292(1), pp. 90–101. doi: 10.1111/imr.12821.

Monson, N. L. *et al.* (2011) 'Rituximab therapy reduces organ-specific T cell responses and ameliorates experimental autoimmune encephalomyelitis', *PLoS ONE*, 6(2), pp. 1–6. doi: 10.1371/journal.pone.0017103.

O'Neill, S. K., Glant, T. T. and Finnegan, A. (2007) 'The role of B cells in animal models of rheumatoid arthritis', *Frontiers in Bioscience*, 12, pp. 1722–1736. Available at: http://ci.nii.ac.jp/naid/40015195484/en/.

Staun-Ram, E. and Miller, A. (2017) 'Effector and regulatory B cells in Multiple Sclerosis', *Clinical Immunology*. Elsevier Inc., 184, pp. 11–25. doi: 10.1016/j.clim.2017.04.014.

Ücal, M. *et al.* (2017) 'Widespread cortical demyelination of both hemispheres can be induced by injection of pro-inflammatory cytokines via an implanted catheter in the cortex of MOG-immunized rats', *Experimental Neurology*. Elsevier Inc., 294, pp. 32–44. doi: 10.1016/j.expneurol.2017.04.014.

Weber, M. S. *et al.* (2010) 'B-cell activation influences T-cell polarization and outcome of anti-CD20 B-cell depletion in central nervous system autoimmunity', *Annals of Neurology*, 68(3), pp. 369–383. doi: 10.1002/ana.22081.

Tables

Table 1 Number of animals per group. The planed animal groups were C1 = 5, E1 = 10, C2 = 5, E2 = 10. We had one animal loss during surgery, resulting in a total animal number of n = 29. There are always catheter losses during the experiment. Those animals changed to the C0 group, since the catheter losses occurred before any cytokine injection and we know from previous work that demyelination only appears when animals receive both MOG immunization and cytokine injection. The catheter losses are also the reason for the unequal partitioning.

Experimental Group		Number of DA rats n =
C0	control, MOG immunized, no cytokine	4
C1	MOG before control antibody	4
E1	MOG before anti-CD20 therapy	10
C2	control antibody before MOG	3
E2	anti-CD20 therapy before MOG	8
In total		**29**

Figures

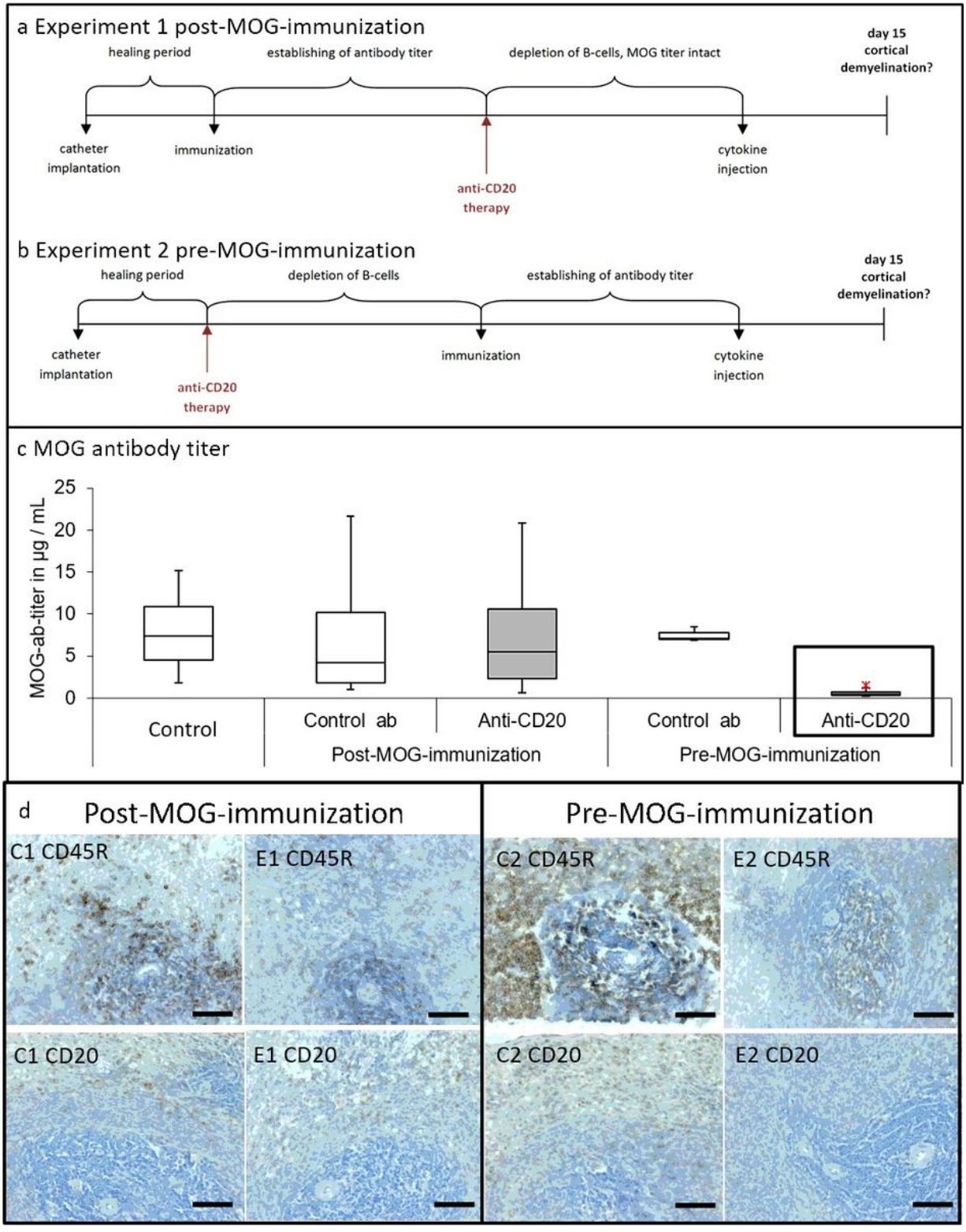

Figure 1

Timelines of the two different experimental approaches, MOG titer of the different experimental groups and immunohistochemical staining of the spleen with two different B-cell markers. Experiment 1 is shown in (a), where B-cell depletion is induced after catheter implantation and immunization. The MOG antibody titer is already established at that time. The hypothesis behind this approach is, that after cytokine injection through the catheter, cortical demyelination in our rats is at least reduced. In (b)

Experiment 2 is schematically illustrated. Rats are treated with anti-CD20 therapy after catheter implantation but before immunization with MOG. The hypothesis is, that after treatment with anti-CD20 antibodies, less or no demyelination is expected. In (c) the MOG titer of the different groups is shown, with the results being in a comparable range with no significant differences in between, except E2. As expected, only the E2 group, highlighted with a rectangle, shows significant differences to the C0 ($p = 0.017$), C2 ($p = 0{,}014$) and E1 ($p = 0.004$). The immunohistochemical stainings (d) show all pictures near lymph follicle, opposed are control groups and experimental groups, respectively. The first line shows CD45R positive cells and the second line represents CD20 positive cells. Both markers show more positive cells in C1 and C2 in comparison to E1 and E2, as expected. Scalebars represent 50 µm.

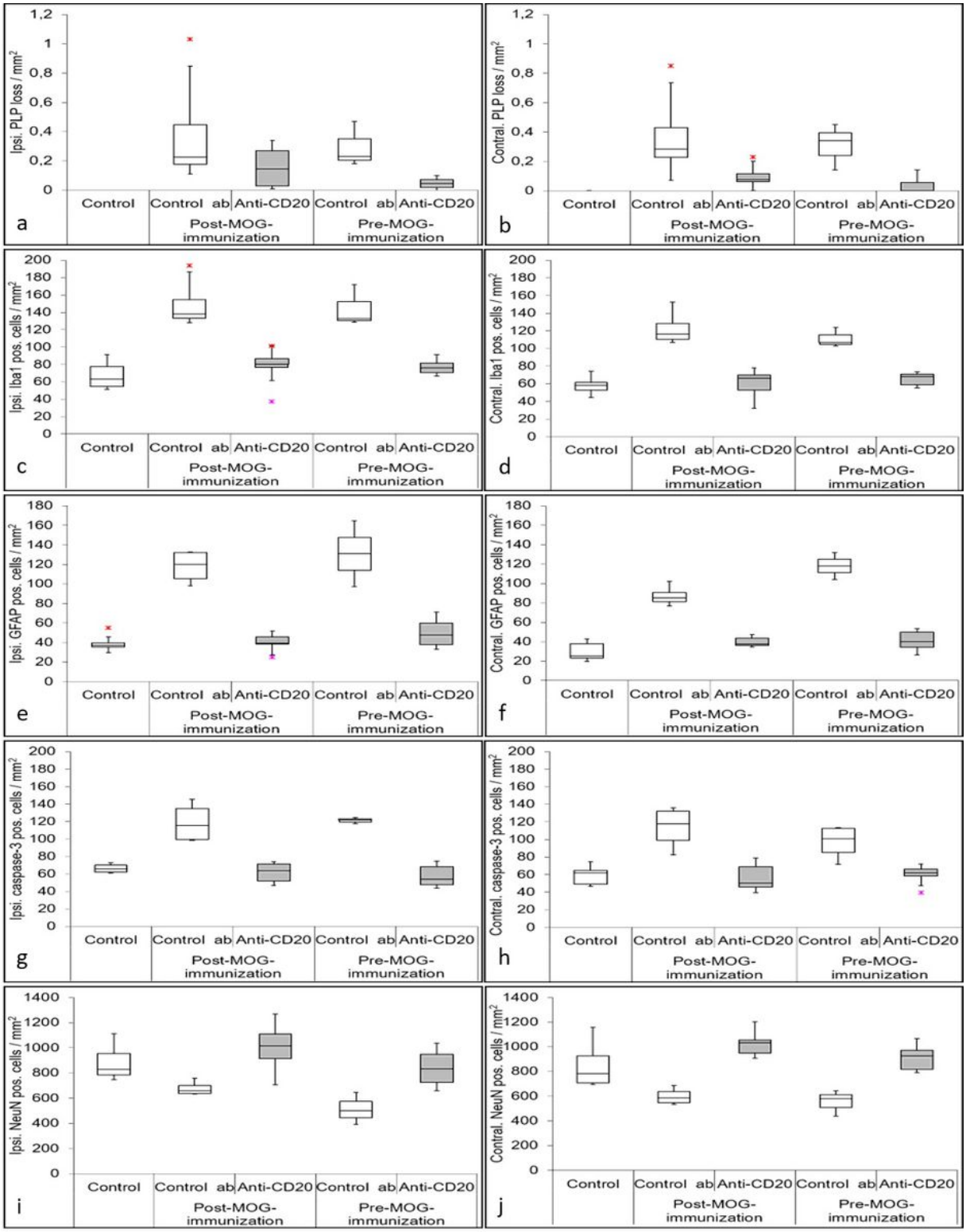

Figure 2

Quantification of cortical demyelination, microglial activation, astrocyte activation, apoptotic cells and neuronal loss. PLP loss is illustrated in (a) on the ipsilateral hemisphere and in (b) on the contralateral hemisphere. Both anti-CD20 therapy approaches result in less PLP loss, with a slightly higher impact of E2. Microglial activation is shown in (c) on the ipsilateral hemisphere and in (d) on the contralateral hemisphere. Both anti-CD20 therapy approaches show less microglial activation compared to the control

groups. The microglial activity is comparable to the C0. Results of activated astrocytes are shown in (e) on the ipsilateral and in (f) on the contralateral side. There are more activated astrocytes detectable in control groups in comparison to the anti-CD20 therapy groups, which are comparable to the C0. Apoptotic cell-counts are illustrated in (g) on the ipsilateral and in (h) on the contralateral side. On both sides, apoptotic cell-counts are reduced compared to the control groups and showed comparable cell counts as determined for the C0s. Quantification of neurons is shown in (i) on the ipsilateral and in (j) on the contralateral hemisphere. Control groups showed higher neuronal loss in comparison to C0s and anti-CD20 therapy groups. In all of those quantifications, there is a significant difference between the C0 and the control groups, but there is no significant difference between C0 and anti-CD20 therapy groups, indicating an overall favorable role of this therapy approach.

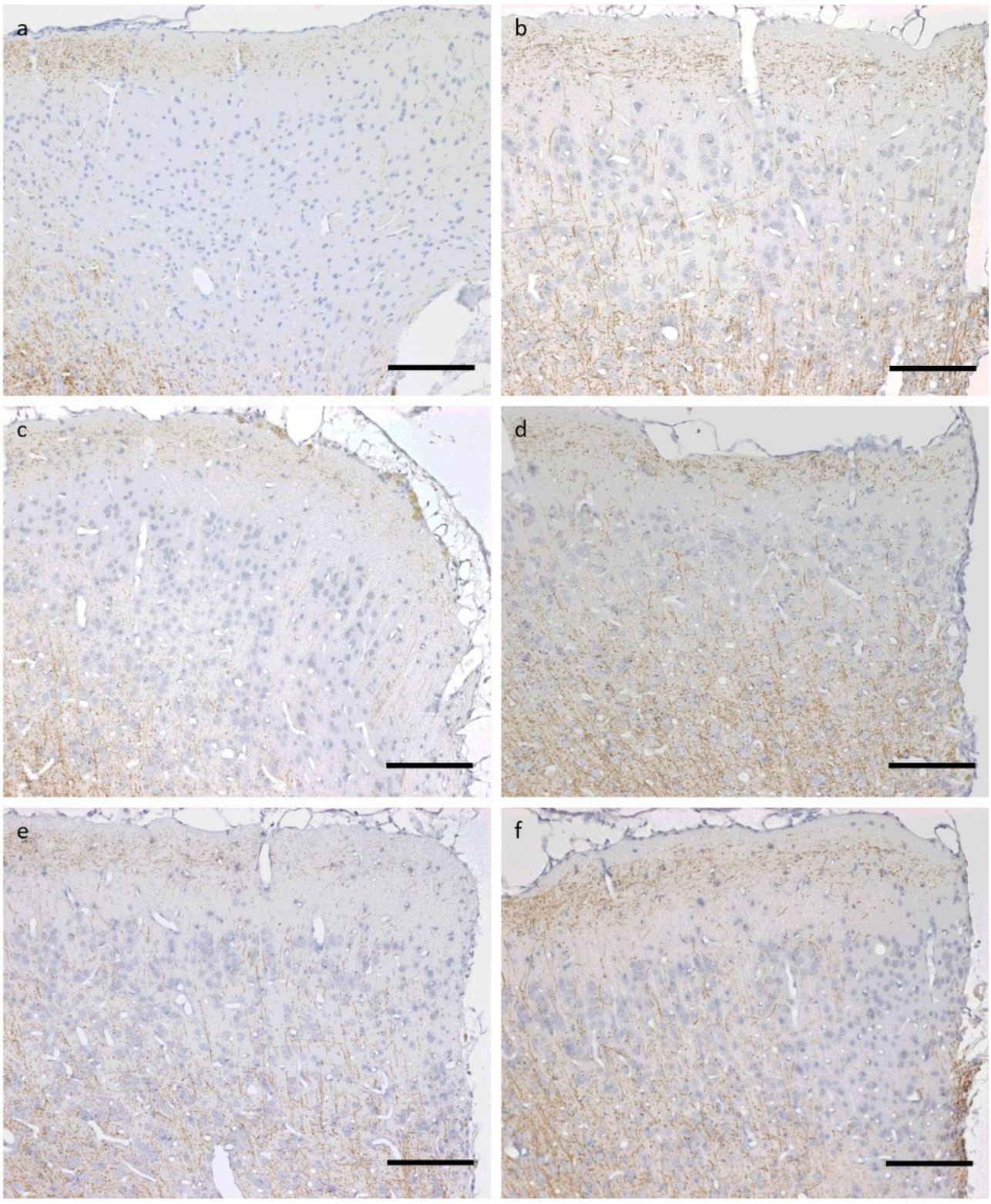

Figure 3

Representative PLP staining comparing the two experimental approaches to C0 and an animal receiving no therapy at all. One upper corner of the catheter puncture side on the ipsilateral hemisphere is shown on each photo. The first line shows the difference between a rat receiving no therapy at all (a) and a C0 (b). In the second line, the C1 group (c) shows more PLP loss than the therapy group E1 (d). This pattern is also comparable in the last line, showing C2 (e) and E2 (f). Scalebars represent 100 µm.

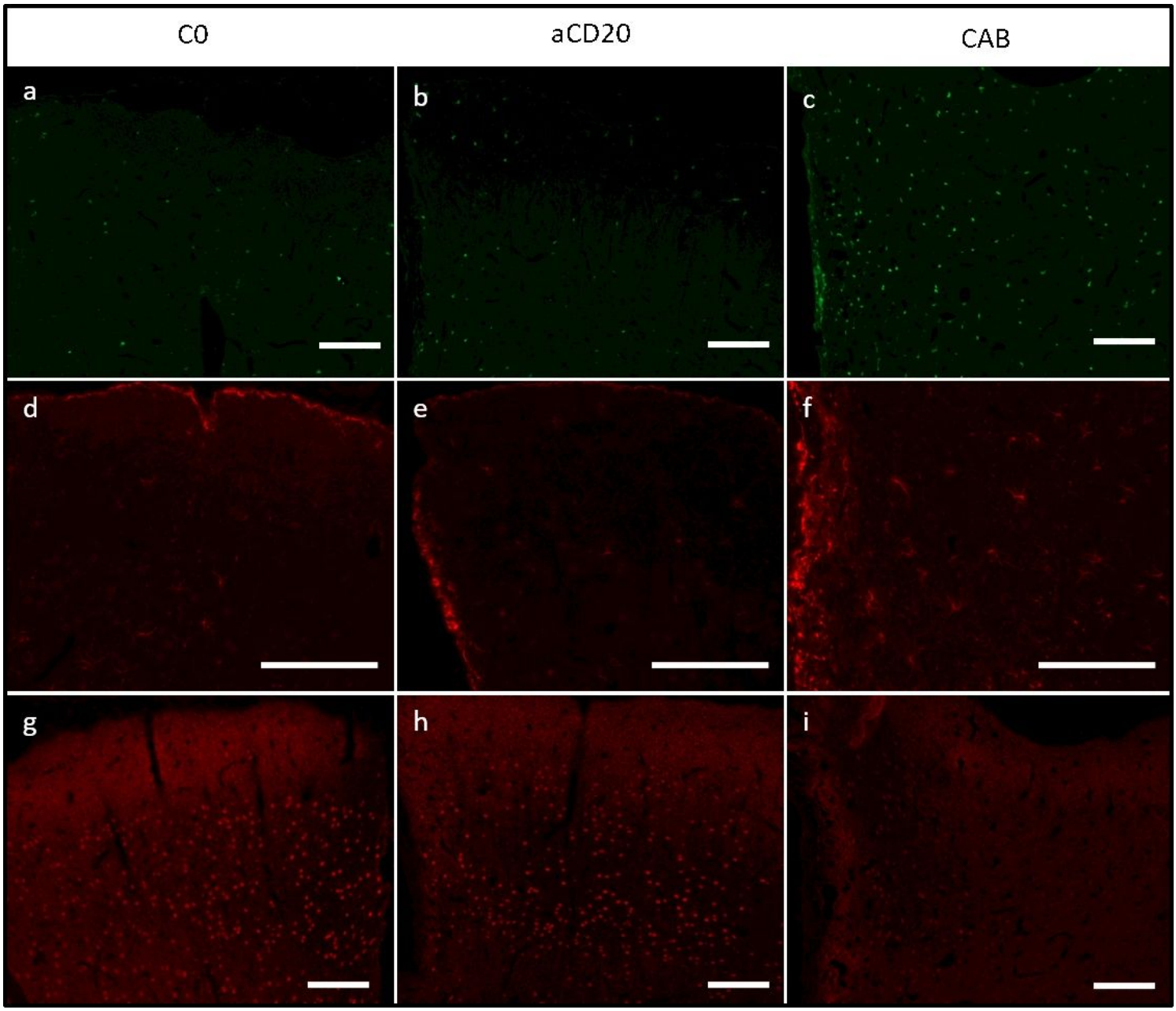

Figure 4

Representative immunofluorescent stainings comparing the therapy groups, control groups and C0. Because of the comparability of the different experimental approaches, only C2/E2 results are shown. The first line shows Iba1 staining, a marker for microglial activation. Microglial activation of C0 (a) is comparable to E2 (b), whereas C2 (c) shows more microglial activation. A similar pattern is detectable when looking at GFAP staining, a marker for activated astrocytes in the second line. Also, C0 (d) and E2 (e) results are comparable and there are more activated astrocytes detectable in C2 (f). The neuronal preservation in E2 (h) is comparable to naïve neuron occurrence (g) but there is neuronal loss detectable in C2 (i). Scalebars represent 100 µm.

Supplementary Files

This is a list of supplementary files associated with this preprint. Click to download.

- Supplementaryfig1.tif
- Supplementarytable12.docx